ChemPubSoc Europe

DOI: 10.1002/ejic.201601470

EurJIC European Journal of Inorganic Chemistry

Full Paper

Bis(heterocyclo)methane Ligands

From Bis(imidazol-2-yl)methanes to Asymmetrically Substituted Bis(heterocyclo)methanides in Metal Coordination

David-R. Dauer,[a] Ingo Koehne,[a] Regine Herbst-Irmer,[a] and Dietmar Stalke*[a]

Dedicated to Professor Dr. Evamarie Hey-Hawkins on the occasion of her 60th birthday

Abstract: As an extension to the known symmetric bis(heterocyclo)methanes containing two identical heterocycles, new asymmetric ligand systems, based on benzoxazole, benzothiazole and 1-methylbenzimidazole, are presented. Furthermore, the syntheses and reactions of two new symmetrically substituted methane derivatives, containing either 1-methylimidazole or 1-methylbenzimidazole, are discussed. In this context, firstly, $(1\text{-MeNCNC}_2H_2)_2CH_2$ and $(1\text{-MeNCNC}_6H_4)_2CH_2$, and secondly, $(NCSC_6H_4)CH_2(NCOC_6H_4)$ and $(NCSC_6H_4)CH_2(1\text{-MeNCNC}_6H_4)$, are used as parent compounds. They can be easily deprotonated at the central methylene bridge to generate a monoanionic structure akin to NacNac, so that the following complexes can be obtained: $[Me_2Al\{(1\text{-MeNCNC}_2H_2)_2CH\}]$, $[Me_2Al\{(1\text{-MeNCNC}_6H_4)_2CH\}]$, $[Me_2Al\{(NCSC_6H_4)CH(NCOC_6H_4)\}]$, $[Me_2Ga\{(NCSC_6H_4)CH(NCOC_6H_4)\}]$, $[Me_2Al\{(NCSC_6H_4)CH(1\text{-MeNCNC}_6H_4)\}]$, $[(THF)_2Li\{(1\text{-MeNCNC}_6H_4)_2CH\}]$ and $[(diox)_2Li\{(NCSC_6H_4)CH(1\text{-MeNCNC}_6H_4)\}]$. These compounds have been fully characterised by single-crystal X-ray diffraction (in the solid state) and NMR spectroscopy (in solution).

Introduction

The first transition-metal complexes of the β-diketiminate (NacNac, **A**; Scheme 1) ligand were mentioned in 1968,[1] and in the past two decades, many β-diketiminate structures containing main-group metals have been synthesised and fully characterised.[2] These complexes embrace aluminium(III), gallium(III) and indium(III) compounds. For aluminium, these range from alkyl- to hydrido- to halido-substituted metal centres. Remarkably, the dialkylaluminium β-diketiminates show catalytic activities similar to those of transition-metal catalysts.[3]

This has sparked interest, and the rising research activity in the broad field of NacNac metal complexes has fuelled the focus on other promising ligand platforms, which are closely related to the ubiquitous β-diketiminato ligand. Most of them mimic its chelating coordination behaviour, so that upon metallation, six-membered metalloheterocycles with six delocalised π-electrons are formed, in which two imine nitrogen atoms are operating as Lewis donors to the metal centre.[4] In this paper, the two RC=NR' moieties of the archetypical NacNac ligand are replaced by fused heterocycles, which also possess an endocyclic C=N imine moiety each, to retain the same coordination abilities (**B** and **C**; Scheme 1).

Another ligand class is launched when two 2-pyridyl moieties are introduced as side arms, instead of the above-mentioned oxazolines (**D**; Scheme 1). With a methylene bridge, the resulting dipyridylmethane[5] and the corresponding methanides were already investigated in the 1990s. As communicated in previous publications, our group synthesised a series of lithium and Group 13 metal complexes of bis(pyrid-2-yl)methanide, and an associated structure–reactivity study was performed on the basis of the results of X-ray diffraction experiments.[6] Representing the Group 1 complexes, $[(12\text{-crown-4})_2Li][Li\{(2\text{-NC}_5H_4)_2CH\}_2]$ can be highlighted as a solvent-separated ion-pair lithium lithiate, or $[(THF)_2Li\{(2\text{-NC}_5H_4)_2CH\}]$ as the related contact ion pair, both solely yielding Li–N contacts.[6a,6c] These two lithiated compounds were easily accessible through deprotonation reactions of the parent dipyridylmethane with equimolar amounts of *n*BuLi in either hexane or THF as the solvent. As an intermediate of that deprotonation, it was possible to isolate the complex $[\{(2\text{-NC}_5H_4)_2CH_2\}Li\{(2\text{-NC}_5H_4)_2CH\}]$ at –80 °C. In this complex,

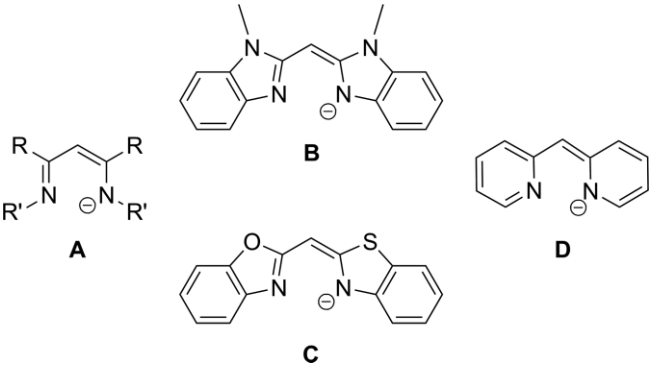

Scheme 1. *N*,*N*-Chelating monoanionic ligands.

[a] *Institut für Anorganische Chemie, Georg-August-Universität Göttingen, Tammannstraße 4, 37077 Göttingen, Germany*
E-mail: dstalke@chemie.uni-goettingen.de
www.uni-goettingen.de/de/53448.html

Supporting information for this article is available on the WWW under http://dx.doi.org/10.1002/ejic.201601470.

only one half of the starting material is deprotonated, whereas the other 0.5 equiv. remains unreacted to give a lithium complex containing one monoanionic and one neutral ligand at the same time.[6b]

Additionally, various Group 13 metal complexes, like $[Me_2Al\{(2\text{-}NC_5H_4)_2CH\}]$ and $[Me_2Ga\{(2\text{-}NC_5H_4)_2CH\}]$, where the $(THF)_2Li$ unit is formally replaced by an Me_2Al or Me_2Ga moiety, were prepared by adding $AlMe_2Cl$ or $GaMe_2Cl$, respectively, to the lithiated compound.[6b,7]

During the past three decades, the bis(heterocyclo)methane ligand systems received little attention in coordination chemistry and were almost forgotten.[8] Although the synthesis of bis(benzothiazol-2-yl)methane has been known for many years,[9] only a few studies have been conducted concerning this interesting ligand. Most of them have presented NMR spectroscopic investigations.[10] They have frequently emphasised the tautomerism of different alkyl-substituted bis(benzothiazol-2-yl)methane derivatives. Others have examined the benzoxazole- and benzimidazole-containing ligands and the derived deprotonated species to estimate the specific charge demands of the heteroaryl substituents.[11] This classification has been largely accomplished by validating ^{13}C and ^{15}N NMR spectroscopic shift/charge ratios, which have been determined for several heteroaromatic and primary organic substituents in related methylene-bridged species.[12] Furthermore, it has been shown that the bis(heterocyclo)methanes are appropriate ligands in transition-metal complexation, because they can act either as neutral ligands LH or as monoanionic ligands L^-.[11a] In the first case, a salt complex $[M(LH)_2]^{2+}$ is obtained by adding divalent transition-metal halides $M^{II}X_2$ to the neutral ligand. In contrast, addition of the corresponding metal acetates $M^{II}(OAc)_2$ gives the deprotonation of the ligand, which yields disubstituted metal complexes $[ML_2]$.

Results and Discussion

Synthesis of the Ligands

Apart from the symmetrically or homodisubstituted bis(heterocyclo)methane derivatives **1** and **2**, the related ligand systems **3** and **4**, containing two different methylene-bridged heteroaromatic side arms, are also part of the investigations within this work. In those ligands, the intrinsic properties of two different benzannulated heteroaryls are combined. Presumably, these hybrid species exhibit new synergistic features in contrast to the comparable symmetrically substituted ligands, which might result in, for example, different metal coordination. In the following paragraphs, the syntheses of **1**–**4**, as well as their derived Group 1 and Group 13 metal complexes **5**–**11**, are described in a comparative approach. In principal, the structural characterisation was accomplished by applying single-crystal X-ray diffraction experiments and in-depth NMR spectroscopic investigations in solution.

On the basis of 1-methylimidazole, the chelating ligand system **1** was synthesised in a two-step procedure. The starting material (2 equiv.) was lithiated with *n*BuLi and reacted in a one-pot synthesis with diethyl carbonate (1 equiv.) as an electrophile. The intermediate ketone derivative **1a** is formed after cleavage of lithium ethanolate and an aqueous workup. To obtain the methylene-bridged ligand **1**, the intermediate **1a** undergoes a classical Wolff–Kishner reduction by reaction with KOH and hydrazine hydrate at elevated temperatures (see Scheme 2). Compound **1** is isolated in a moderate, but suitable, overall yield of 43 %.

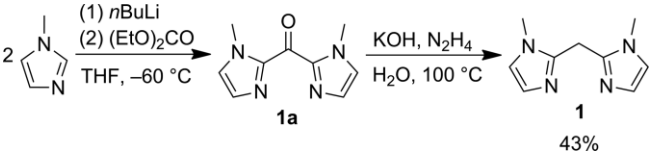

Scheme 2. Synthesis of bis(1-methylimidazol-2-yl)methane **1**.

The related benzannulated species **2** was prepared by another synthetic approach, as shown in Scheme 3: different from **1**, in this case, the five-membered imidazole heterocycles have to be generated in the same step, as the coupling is accomplished through the methylene bridge. As appropriate starting materials, *N*-methylphenylenediamine (2 equiv.) and diethyl malonate (2 equiv.) were used. The malonic acid derivative serves as a C_3 building block, which enables the cyclocondensation reaction to give the imidazole moieties and to introduce the required CH_2 bridge. The reaction is performed in half-concentrated aqueous hydrochloric acid (boiling) to facilitate the ongoing cyclisation reaction, and so, the crude ligand **2** is isolated by the addition of ammonia to initiate precipitation. Rigorous purification by column chromatography gives a yield of 26 %.

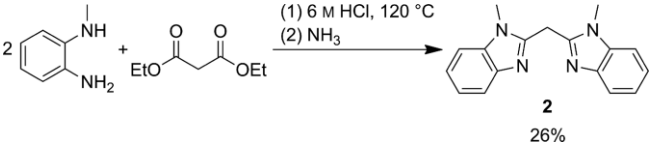

Scheme 3. Synthesis of bis(1-methylbenzimidazol-2-yl)-methane **2**.

The crystal structures of **1** and its benzo-annulated derivative **2** were determined and are depicted in Figures 1 and 2, respectively, and structural data are given in Table 1. The *N*-methyl groups and the corresponding imine nitrogen atoms on the other side of the specific heterocycle in both compounds are quite differently orientated. While in **1** the methyl groups are pointing almost in opposite directions, this twisting is not as pronounced in **2**. The main reason for this difference is the absence of the aromatic C_6 perimeter. In **1**, two hydrogen atoms next to the imine nitrogen atoms are available for hydrogen bonding, but are missing in **2**. They are prone to building up three-dimensional networks of hydrogen bonds to neighbouring imine nitrogen atoms due to the distinct polarisation of the C–H bonds adjacent to the endocyclic heteroatoms. Therefore, two different hydrogen bonds are present in the solid state of **1**: one is rather strong and refers to the N2···H3 distance of 2.468 Å and the corresponding N2···H3–C3 angle of 151.5°. The second one seems to be less stable, due to the increased N2···H4 distance of 2.649 Å, even though the corresponding

N2···H4–C4 angle (156.0°) is slightly closer to favourable linearity.[13]

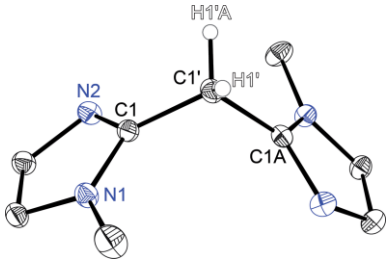

Figure 1. Molecular structure of (1-MeNCNC$_2$H$_2$)$_2$CH$_2$ (**1**). Anisotropic displacement parameters are depicted at the 50 % probability level. C–H hydrogen atoms are omitted for clarity, except those on the bridging carbon atom. Structural data are given in Table 1.

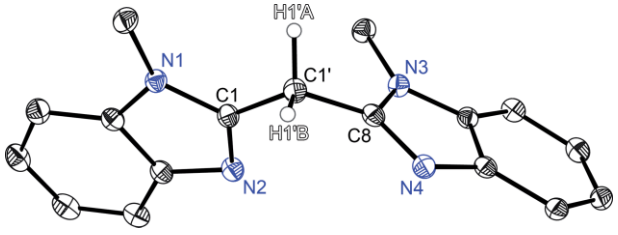

Figure 2. Molecular structure of (1-MeNCNC$_6$H$_4$)$_2$CH$_2$ (**2**). Anisotropic displacement parameters are depicted at the 50 % probability level. C–H hydrogen atoms are omitted for clarity, except those on the bridging carbon atom. Structural data are given in Table 1.

Table 1. Selected bond lengths [Å] and angles [°] for the ligands **1** and **2**.

	1	**2**
C1–C1′, C8–C1′	1.5018(14)	1.4984(15), 1.4911(14)
C1–N2, C8–N4	1.3254(15)	1.3154(14), 1.3166(15)
C1–C1′–C1A/C8	111.97(13)	113.54(9)

The syntheses of the parent ligand systems **3** and **4** are depicted in Scheme 4. A two-step procedure was employed to connect two different benzo-annulated heterocycles to a bridging methylene moiety. First, malonic dinitrile (1 equiv.) is treated with *ortho*-aminothio-phenol (1 equiv.) to give the mono-(benzothiazol)-substituted methane derivative (analogous to the procedure depicted in Scheme 2) that provides one nitrile group for the introduction of a second heterocycle. In the second step, the corresponding *ortho*-substituted aniline derivative (*ortho*-aminophenol or *N*-methylphenylenediamine) is added, which undergoes a cyclocondensation reaction with 2-(benzothiazol-2-yl)acetonitrile to give the second heterocycle. This reaction takes place at elevated temperatures of 180 °C in the presence of polyphosphoric acid (PPA) as the solvent under vigorous stirring for several hours. After aqueous workup and purification, the two different ligand systems **3** and **4**, which differ by only the benzoxazole or benzimidazole unit, can be obtained in yields of 89 % and 48 %, respectively.

As a side product in the synthesis of **3**, the amide 2-(benzothiazol-2-yl)-*N*-(2-hydroxyphenyl)acetamide **3a** could also be isolated by column chromatography. It is characterised by NMR spectroscopy and single-crystal X-ray determination. Compound **3a** can be envisaged as an intermediate species that occurs while generating the benzoxazole moiety in **3**. After the first nucleophilic attack of the amine nitrogen atom on the positive-polarised nitrile carbon atom, a primary imine is formed temporarily, which is then attacked by the hydroxy group to give a five-membered heterocycle. Because of insufficient reaction time, the cyclisation reaction was not fully completed, so that some amount of the primary imine remained, which was hydrolysed by the aqueous workup to give **3a** (Figure 3 and Table 2).

The asymmetrically substituted methane derivative **3** crystallises in the triclinic space group $P\bar{1}$, and the asymmetric unit contains one complete molecule. Due to the very slight differences of the benzoxazole and benzothiazole moiety, there is no preferred orientation of those residues in the solid state. However, this positional disorder could be deconvoluted, and the structure was refined satisfactorily. This problem of the disordered heterocyclic substituents is omnipresent in the other determined structures containing asymmetric ligands, but can be tackled successfully (vide infra).

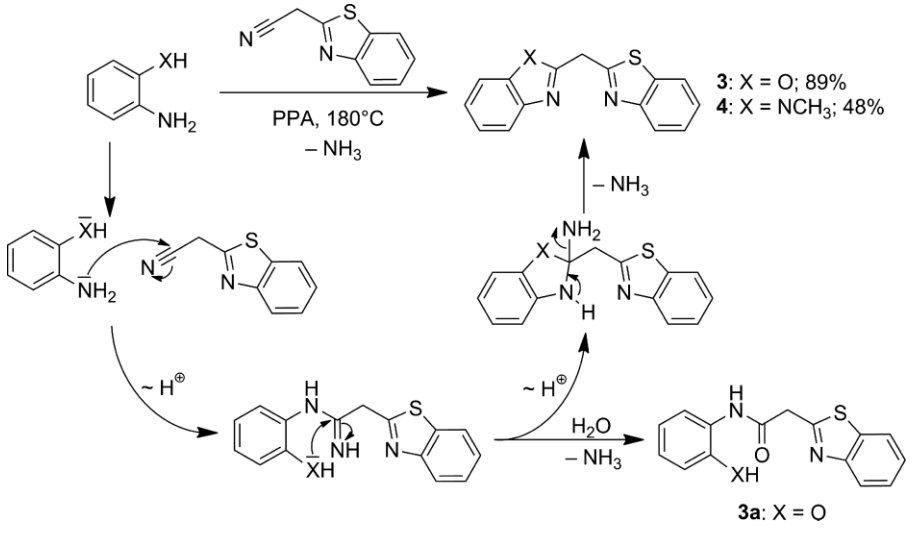

Scheme 4. Synthesis route to the asymmetric bis(heterocyclo)methanes **3** and **4**.

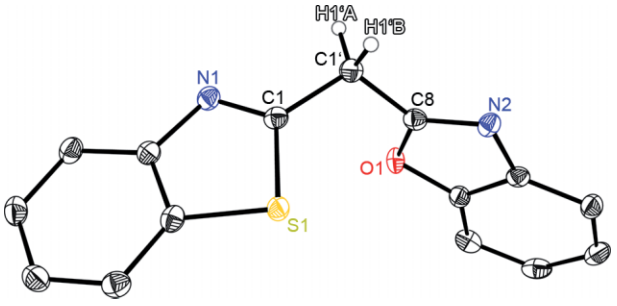

Figure 3. Molecular structure of $(NCSC_6H_4)CH_2(NCOC_6H_4)$ (**3**). Anisotropic displacement parameters are depicted at the 50 % probability level. Positional disorder and C–H hydrogen atoms are omitted for clarity, except those on the bridging carbon atom. Structural data are given in Table 2.

Table 2. Selected bond lengths [Å] and angles [°] for the ligand species **3** and **4**. Due to the presence of two molecules in the asymmetric unit of **4**, two values are given.

	3	**4**
C1–C1′	1.5034(18)	1.503(4); 1.516(4)
C1–N1	1.2929(17)	1.304(3); 1.296(3)
C1–C1′–C8	112.87(11)	111.0(2); 110.2(2)
H1′···N3	–	2.03(2)
H3′···N3A	–	2.06(2)
H2′···O2	–	1.90(2)
H4′B···O1	–	1.92(3)
O1–H1′···N3	–	168(3)
O2–H3′···N3A	–	173(4)
O1–H2′···O2	–	178(3)
O2B–H4′B···O1	–	163(5)

The same is valid for the imidazole and thiazole moiety in the crystal structure of the related ligand **4**, which carries a *N*-methylbenzimidazole unit instead of the benzoxazole substituent in **3**. Compound **4** crystallises in the chiral monoclinic space group $P2_1$, and two target molecules (together with two water molecules) can be found in the asymmetric unit. These water molecules originate from the aqueous ethanol solution used in the recrystallisation process of the ligand and are incorporated in an interesting hydrogen-bonding network (Figure 4 and Table 2).

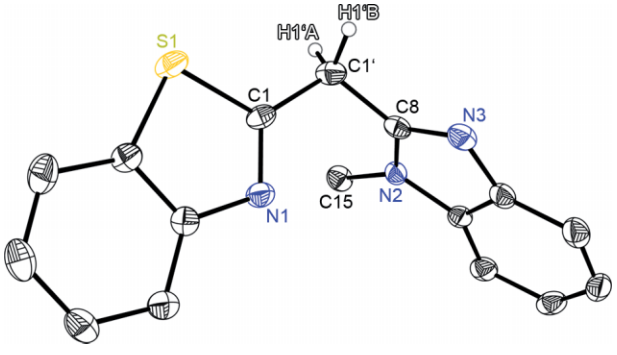

Figure 4. Molecular structure of one molecule of $(NCSC_6H_4)CH_2$(1-Me-$NCNC_6H_4$) (**4**). Anisotropic displacement parameters are depicted at the 50 % probability level. Positional disorder and C–H hydrogen atoms are omitted for clarity, except those on the bridging carbon atom. Structural data are given in Table 2.

The water molecules form a hydrogen-bonded chain in the solid state, with every second molecule further linked to two neighbouring parent ligands through the endocyclic imine nitrogen atoms. Each oxygen atom acts as a double hydrogen donor (O–H···O and O–H···N) and as a single hydrogen acceptor from the previous water molecule (O···H–O) (see Figure 5).

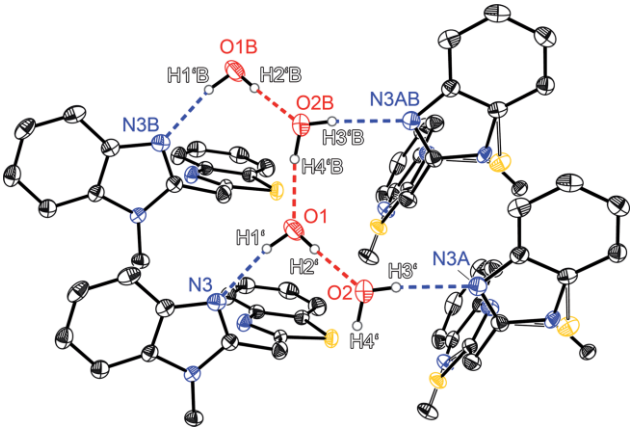

Figure 5. Hydrogen-bonding pattern of $(NCSC_6H_4)CH_2$(1-Me-$NCNC_6H_4$) (**4**). Structural data are given in Table 2.

Synthesis of the Metallated Species

The next synthetic step covers the various metallation reactions that were applied to the discussed ligand systems. As depicted in Scheme 5, the synthesis of the metallated species was accomplished by adding the neat organometallic reagent ($AlMe_3$ or $GaMe_3$, 1.1 equiv.) or an organic solution of *n*BuLi to **1**, **2**, **3** and **4**, which were either dissolved in toluene as a nonpolar solvent or 1,4-dioxane as a polar donor solvent. After complete addition, the reaction mixture was stirred for several hours overnight to complete full conversion. The reaction of **1** and $AlMe_3$ yields the methanide derivative **5**. By using recrystallisation from toluene, suitably diffracting crystals could be obtained, which afforded the corresponding molecular structure shown in Figure 6. A NacNac-like coordination motif is observed, in which both imine nitrogen atoms act as electron donors to chelate the implemented metal fragment after deprotonation. In our earlier papers, benzo-annulated methanide and amide derivatives could be obtained and structurally characterised, though those complexes consist of a ligand backbone substituted twice with the same benzo-annulated heterocycle. For the benzo-annulated **6**, unfortunately no suitable crystals could be grown due to the needle-like shape, which is responsible for weak X-ray scattering. Nevertheless, this dimethylaluminium species **6** was appropriately characterised in solution by using ^1H and ^{13}C NMR spectroscopy.

The aluminium compound **7**, derived from the neutral ligand system **3**, crystallises in the monoclinic space group $P2_1/c$, and the asymmetric unit contains one target molecule (Figure 7). As in the parent ligand system **3**, positional disorder also occurs in **7**, because in the solid state, no favoured orientation (neither of the benzoxazole nor of the benzothiazole moiety) is attained. Again, this disorder leads to a slight unreliability of the determined bond lengths and angles within this structure, because

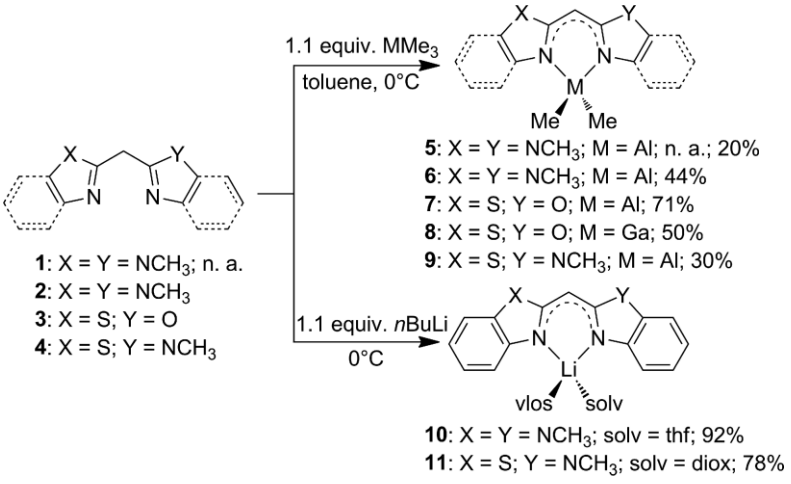

Scheme 5. Metallation reactions of the bis(heterocyclo)methanes **1**–**4** (n.a.: not annulated).

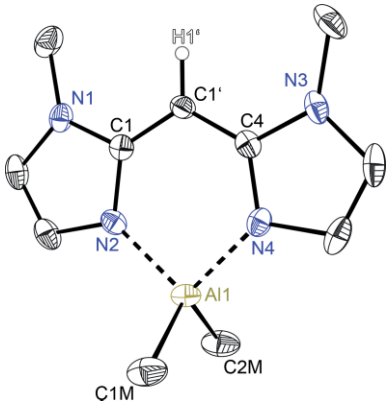

Figure 6. Molecular structure of $[Me_2Al\{(1\text{-}MeNCNC_2H_2)_2CH\}]$ (**5**). Anisotropic displacement parameters are depicted at the 50 % probability level. C–H hydrogen atoms are omitted for clarity, except for that on the bridging carbon atom.

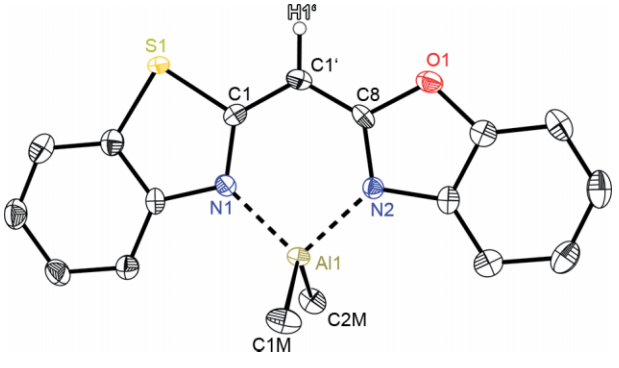

Figure 7. Molecular structure of $[Me_2Al\{(NCSC_6H_4)CH(NCO\ C_6H_4)\}]$ (**7**). Anisotropic displacement parameters are depicted at the 50 % probability level. Positional disorder and C–H hydrogen atoms are omitted for clarity except for that on the bridging carbon atom. Structural data are given in Table 3.

of the two differently oriented molecules, which are rotated by about 180° with respect to each other. Hence, no detailed discussion concerning the bond lengths and angles within the heterocycles will be given. Only the unambiguous values for the bite angle, the N–M distances and the displacement of the metal atom from the chelating C_3N_2 plane are discussed for all metallated species (see Table 3).

The distorted tetrahedral coordination geometry of Al1 in **7** results in averaged Al–N distances of 1.924 Å, a bite angle of 93.43° and a slight dislocation of the Al^{3+} cation from the chelating C_3N_2 plane of about 0.053 Å. In comparison with previous work on related bis(heterocyclo)methanide ligand systems like $[(NCSC_6H_4)_2CH]^-$ or $[(NCOC_6H_4)_2CH]^-$, which contain two identical benzoxazole or benzothiazole substituents, respectively, the obtained values for the dimethylaluminium species range between those of the complexes $[Me_2Al\{(NCOC_6H_4)_2CH\}]$[4a] [Al–N 1.91(20) Å; N–Al–N 91.76(9)°] and $[Me_2Al\{(NCSC_6H_4)_2CH\}]$[4a] [Al–N 1.92(14) Å; N–Al–N 94.78(6)°], but notably, **7** is closer to the bis(benzothiazol-2-yl)methanide derivative.

The crystal structure of the second dimethylaluminium-containing complex **9**, could be refined successfully, despite the positional disorder. Again, the metal cation is coordinated exclusively by the ring-imine nitrogen donor atoms and the two methyl groups in a distorted tetrahedral fashion. The dislocation of the Al^{3+} cation from the chelating C_3N_2 plane, compared with **7**, is five times larger. The parent ligand system **4** is a hybrid between the bis(benzothiazol-2-yl)methane and the bis(1-methylbenzimidazol-2-yl)methane ligand **2**. Unfortunately, the solid-state structure of the corresponding dimethylaluminium complex $[Me_2Al\{(1\text{-}MeNCNC_6H_4)_2CH\}]$ (**6**) could not be obtained, due to hampered crystallisation. However, the values of $[Me_2Al\{(NCSC_6H_4)_2CH\}]$[4a] [Al–N 1.9233(14) Å; N–Al–N 94.79(6)°] compare with those expected for **9**.

Table 3. Selected bond lengths and angles for the metallated species **7**–**9** and **11**.

	7	**8**	**9**	**11**
M–N (mean) [Å]	1.924	1.993	1.911	1.954
N–M–N [°]	93.43(11)	91.3(3)	94.3(3)	97.0(2)
Deviation of M from the C_3N_2 plane [Å]	0.053(3)	0.289(7)	0.240(5)	0.018(12)

In addition to the aluminium complexes, the higher homologue, containing the $GaMe_2$ moiety in **8**, and the lithium complexes **10** and **11** could be investigated by X-ray diffraction experiments (Figures 8 and 9).

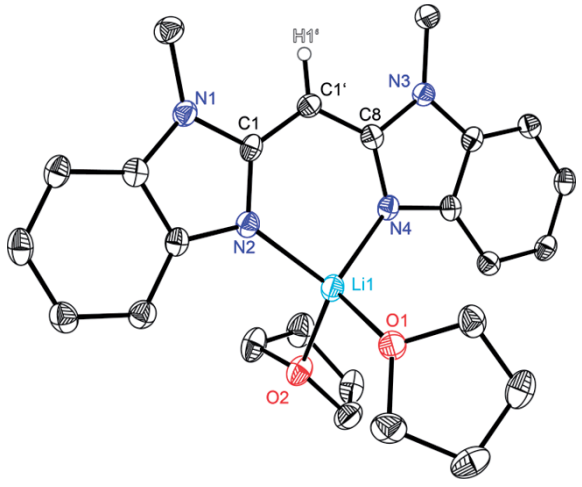

Figure 8. Molecular structure of $[(THF)_2Li\{(1\text{-}MeNCNC_6H_4)_2CH\}]$ (**10**). Anisotropic displacement parameters are depicted at the 50 % probability level. Positional disorder and C–H hydrogen atoms are omitted for clarity except for that on the bridging carbon atom.

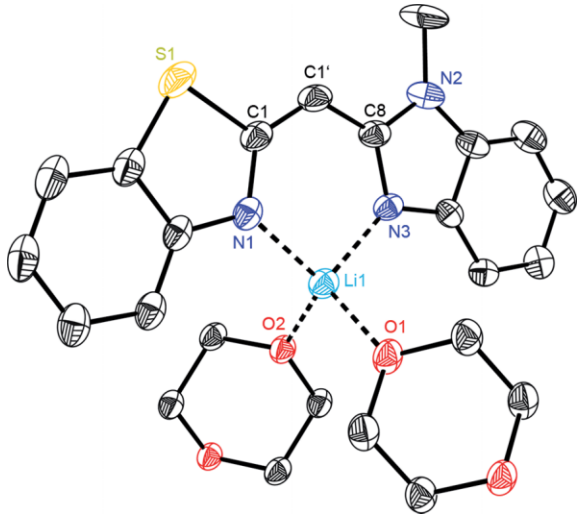

Figure 9. Molecular structure of $[(diox)_2Li\{(NCSC_6H_4)CH(1\text{-}MeNCNC_6H_4)\}]$ (**11**). Anisotropic displacement parameters are depicted at the 50 % probability level. Positional disorder and C–H hydrogen atoms are omitted for clarity. Structural data are given in Table 3.

Compound **8** almost perfectly matches the values found in $[Me_2Ga\{(NCOC_6H_4)_2CH\}]$[4a] [Ga–N 1.996(20) Å; N–Ga–N 89.2(2)°] and $[Me_2Ga\{(NCSC_6H_4)_2CH\}]$[4a] [Ga–N 1.994(13) Å; N–Ga–N 92.99(8)°] for either side of the substituents. The lithiated species **11**, also derived from the asymmetrically substituted ligand **4**, compares nicely with compound **10**, a similarly bis(heterocyclo)methanide-substituted complex. The main difference between those structures is the donating solvent (THF in **10** and dioxane in **11**). The determined N1–Li1–N3 bite angle of 97.0° and the C1–C1′–C8 backbone angle of 124.6° in **11** are quite similar to the related values in $[(THF)_2Li\{(1\text{-}MeNCNC_6H_4)_2CH\}]$ (**10**; 96.9° and 124.3°). The O1–Li1–O2 angle is 99.6° in **11**, whereas that angle is much wider in the homodisubstituted imidazole compound **10** (mean 111.5°). The observed decreased O1–Li1–O2 angle and Li···ligand plane distance in **11** are presumably caused by the higher steric demand of the dioxane molecules and the resulting coordination polymer in **11**, which reduces that angle and forces the lithium cation more into the plane of the metalloheterocycle.

The comparison with the literature-known lithiated bis(pyrid-2-yl)methanide species $[(THF)_2Li\{(2\text{-}NC_5H_4)_2CH\}]$[6a] also quarries some similarities. The average Li–N distance is 1.97 Å and the bite angle is 96.4°, while the O1–Li1–O2 angle involving the donating THF molecules is 98.9°.[6a,6c,14] Furthermore, the lithium cation is almost ideally placed within the plane of the metalloheterocycle, also seen for the asymmetrically substituted methanide compound **11**.

NMR Spectroscopic Investigations

The ^1H NMR spectrum of the dimethylaluminium complex **7** is shown in Figure 10. Besides the two singlets at δ = –0.45 and 5.76 ppm for the methyl groups on the aluminium atom and the remaining proton on the bridging carbon atom, respectively, the multiplets in the aromatic region of the spectrum show a distinct coupling pattern. Due to the fact that both side arms only differ by the chalcogen ring atom (oxazole or thiazole), the hydrogen atoms on the annulated benzene perimeters exhibit slightly different chemical shifts. The reasonable resolution of the recorded spectrum allows the determination of the underlying coupling constants, which can be derived from the observed multiplets. Each aromatic proton couples to three other protons of the corresponding heterocycle, resulting in a ddd coupling pattern. With the terminal hydrogen atoms H3, H6 or H10, H13, the relatively large ^3J coupling constant towards the *ortho*-protons, as well as the smaller ^4J coupling constants for the *meta*-protons and ^5J coupling constants for the *para*-protons, could be identified. The other protons H4, H5 or H11, H12 show two large ^3J couplings to both neighbouring protons in the *ortho*-position and a smaller ^4J coupling towards the remaining proton in the *meta*-position. By the application of these values, and with the assistance of other 2D NMR spectroscopic experiments like ^1H, ^{13}C HSQC and HMBC, it was possible to properly assign the observed signals in the aromatic region. The exact assignment of these sometimes partially or completely superimposed signals is magnified in the upper part of Figure 10. Notably, the resonance signal of the terminal hydrogen atom H3 is the most downfield-shifted (δ = 7.69 ppm), whereas that of the neighbouring H4 is the most upfield-shifted (δ = 7.19 ppm) with respect to the considered aromatic area. This fact can also be observed in the recorded ^1H NMR spectra of the metallated species **6**, **8** and **9** (vide infra).

The resulting ^1H NMR spectrum of **8**, in which the aluminium cation is replaced by its higher congener gallium, is displayed in Figure 11; it shows certain similarities to the spectrum of the above-mentioned **7**. There is also a singlet at δ = –0.03 ppm for the dimethylgallium moiety and another one for the deprotonated methylene bridge at δ = 5.58 ppm. The region of the aromatic protons covers a range similar to that for **6** (δ = 7.65–

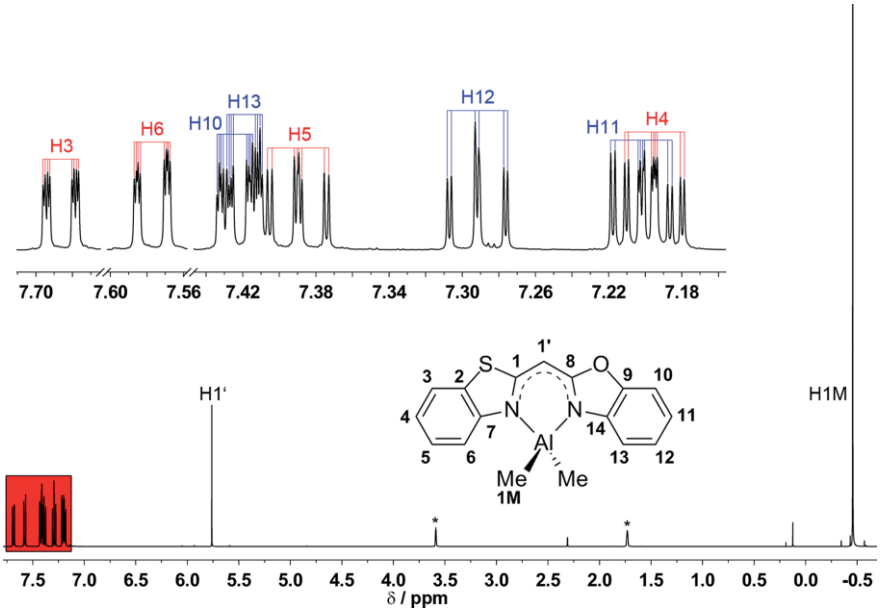

Figure 10. ^{1}H NMR spectrum of **7** (500 MHz, [D$_8$]THF, room temperature; solvent signals are highlighted with *).

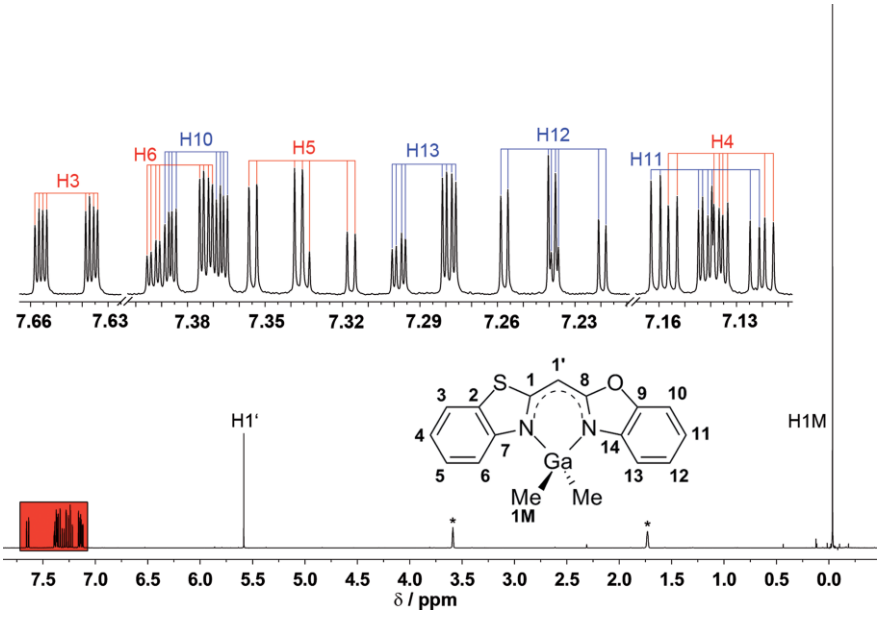

Figure 11. ^{1}H NMR spectrum of **8** (400 MHz, [D$_8$]THF, room temperature; solvent signals are highlighted with *).

7.13 ppm), which again is determined by the chemical shifts of the protons H3 and H4. In analogy to the assignment in **7**, the observed signals could be matched to their correct positions (see magnification in Figure 11), because – in this case – the resolution and separation of the signals is even more advantageous for gaining reliable coupling constants.

For a better comparison of the chemical shifts regarding the parent ligand **3** and the two Group 13 metal complexes **7** and **8**, Figure 12 shows the ^{1}H NMR spectra (focussed on the signals in the aromatic region). Deprotonation and subsequent metallation of **3** shifts the resonance signals of the aromatic protons significantly towards higher field, because the generated lone pair and negative charge of the whole ligand backbone causes a higher electronic shielding of the protons. This effect is more pronounced in the gallium species **8** than in the aluminium complex **7**. With respect to the parent CH_2 bridge or the CH linker, respectively, upon deprotonation of that position, the corresponding resonance signal in both cases is significantly shifted downfield in the ^{1}H and ^{13}C NMR spectroscopic experiments. Compound **3** resonates at δ = 4.85 ppm/34.38 ppm for H1′ and the connected C1′, while metallation results in chemical shifts of δ = 5.76 ppm/71.35 ppm in **7** and 5.58 ppm/70.09 ppm in **8**.

To emphasise the differences in the spectra of the aluminium compound **7** and the gallium compound **8**, the signals of the four terminal protons H3, H6 and H10, H13 have to be highlighted. The protons H6 and H13 seem to be most sensitive to the change of the coordinated metal cation, because they are

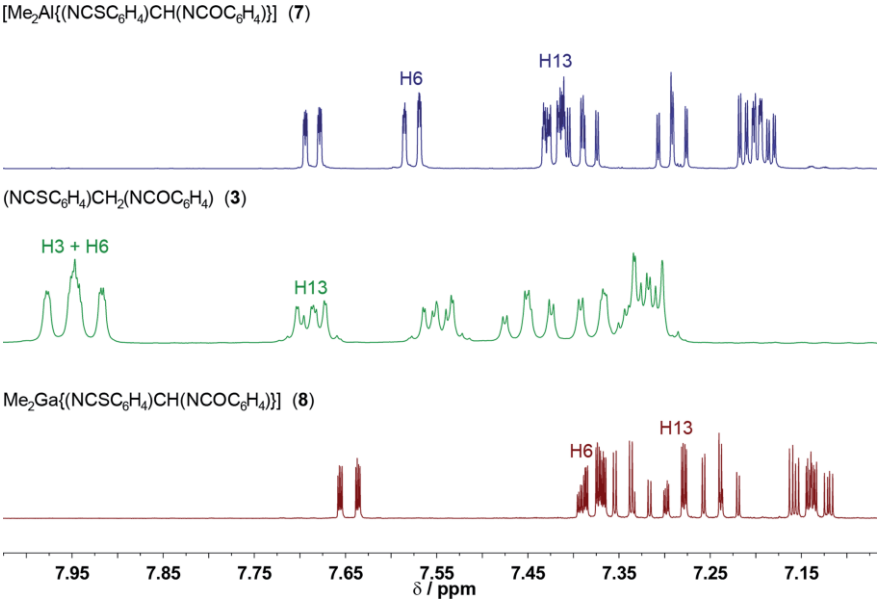

Figure 12. ^{1}H NMR spectra of the parent ligand system **3** (in green), the aluminium complex **7** (in blue) and the gallium complex **8** (in red). For clarity reasons, only the aromatic region is displayed.

pointing directly towards the chelated metal centre, whereas H3 and H10 are pointing to the opposite direction and are therefore less affected by the metal atom. In the parent ligand **3**, the protons H3 and H6 show quite a similar chemical shift, but after metal coordination, the signals of those protons are influenced in a different manner. In **7** and **8**, the change in the chemical shifts referring to the protonated ligand is more pronounced for the inwardly pointing protons H6 (**7**: $\Delta\delta$ = 0.37 ppm; **8**: $\Delta\delta$ = 0.56 ppm) and H13 (**7**: $\Delta\delta$ = 0.27 ppm; **8**: $\Delta\delta$ = 0.40 ppm) than for the outwardly arranged ones H3 (**7**: $\Delta\delta$ = 0.26 ppm; **8**: $\Delta\delta$ = 0.30 ppm) and H10 (**7**: $\Delta\delta$ = 0.13 ppm; **8**: $\Delta\delta$ = 0.17 ppm). On the basis of these differences, it can be assumed that the size of the coordinated metal ion has quite a significant impact on the chemical shifts of the protons H6 and H13. Due to the larger ionic radius and more closed electron shells of the Ga^{3+} cation, in contrast to the Al^{3+} cation, these two protons experience a higher electronic shielding in the case of **8** than that of **7**, causing the corresponding resonances to be shifted more upfield.

Similar observations can be found in the second ligand system **4**, in which the benzoxazole moiety of **3** is formally replaced by an *N*-methylbenzimidazole residue. With this ligand, two metallated species could also be synthesised, but in contrast to the afore-mentioned ligand system, here, a dimethylaluminium-containing complex **9** and a lithiated compound **11** donated by the Lewis base 1,4-dioxane are compared. The recorded ^{1}H NMR spectra of those three compounds are displayed in Figure 13. The differences of the resonance signals of

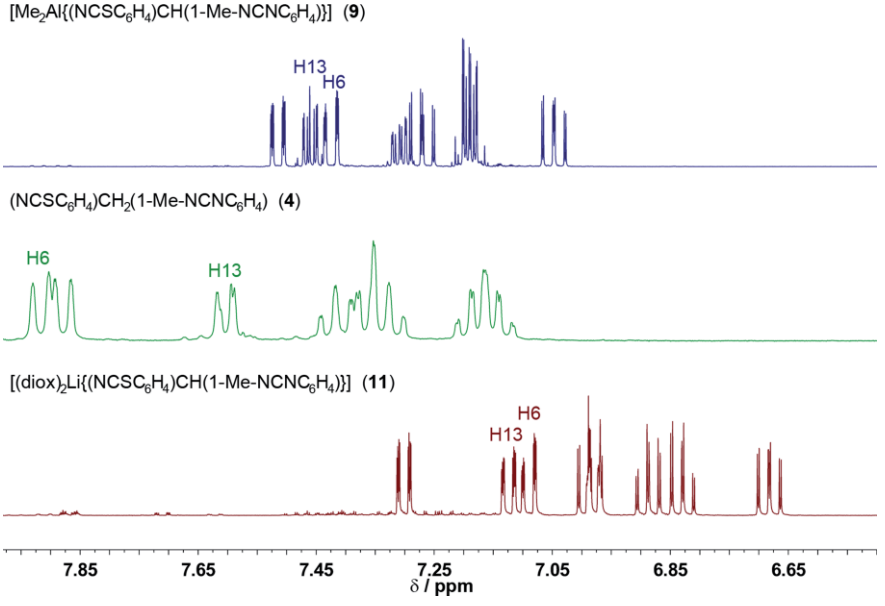

Figure 13. ^{1}H NMR spectra of the parent ligand system **4** and the metallated species **9** and **11**; for clarity reasons, only the aromatic region is displayed.

H6 (**9**: $\Delta\delta$ = 0.49 ppm; **11**: $\Delta\delta$ = 0.83 ppm) and H13 (**9**: $\Delta\delta$ = 0.13 ppm; **11**: $\Delta\delta$ = 0.48 ppm) are significantly larger than those of H3 (**9**: $\Delta\delta$ = 0.36 ppm; **11**: $\Delta\delta$ = 0.58 ppm) and H10 (**9**: $\Delta\delta$ = 0.05 ppm; **11**: $\Delta\delta$ = 0.39 ppm). These results correlate with the observations made before that the protons on the side of the coordinated metal ion interact more with the coordinated fragment. Furthermore, it is evident that the changes of the observed chemical shifts are higher in the case of the lithiated species **11**. This observation was expected due to the increasing ionic radii of the involved metal cations (0.39 Å for Al^{3+}, 0.47 Å for Ga^{3+} and 0.59 Å for Li^{+}), with each in fourfold coordination.[14] As in **7**, the cationic radius of Li^{+} is larger than that of Al^{3+}, and therefore, the signals of the inner protons H6 and H13 are shifted more upfield in lithium complex **11** than in **9**. In contrast to **7** and **8**, the observed coupling pattern of **9** is partially more complex. The protons on the benzimidazole moiety do not show distinct ddd structures, but rather signals of higher orders, so that the coupling constants are not so easily accessible. However, the spectrum at the bottom of Figure 13 again shows a first-order splitting pattern for both moieties (benzothiazole and benzimidazole) due to the chemical-shift difference between the coupled protons being much larger than the coupling constant.

Conclusion

Compounds **1**–**4** were successfully introduced as new non-annulated and benzo-annulated bis(heterocyclo)methane ligands, respectively. In contrast to species **1** and **2**, which are examples of homodisubstituted methanes, the ligand systems **3** and **4** exhibit two different benzo-annulated heterocycles connected to the bridging methylene moiety. All ligand systems were successfully used to synthesise new Group 13 (Al, Ga) (**5**–**9**) and/or Group 1 (Li) (**10** and **11**) metal complexes through concerted deprotonation metallation reactions. All presented compounds were fully characterised and extensively studied by single-crystal X-ray structure determination and solution NMR spectroscopic techniques.

Experimental Section

Procedures: All manipulations were carried out under N_2 or Ar by using Schlenk techniques.[15] All solvents used within the metallation reactions were distilled from Na or K before use. The starting materials were purchased commercially and were used as received. ^{1}H, ^{7}Li, ^{13}C, ^{15}N and ^{27}Al NMR spectroscopic data were recorded with a Bruker Avance 500 MHz, a Bruker Avance 400 MHz or a Bruker Avance 300 MHz spectrometer, and they were referenced to the deuterated solvent ([D_8]THF or [D_6]DMSO).[16] Elemental analyses (C, H, N and S) were carried out with a Vario EL3 at the Mikroanalytisches Labor, Institut für Anorganische Chemie, University of Göttingen. Several compounds contain lattice solvent, as confirmed by X-ray diffraction data, because the crystals were grown in the mother liquor. As a result of drying these samples, the whole amount of incorporated lattice solvent could not be removed, so that no solvent-free compounds were obtained. The remaining solvent led to slightly enhanced values in the elemental analyses for C and H. All EI mass spectra (70 eV) were recorded with a Finnigan MAT95.

Ligand Syntheses

(1-MeNCNC$_2$H$_2$)$_2$CO (1a): A solution of *n*BuLi (2.15 M in hexane, 46.5 mL, 100 mmol, 2.0 equiv.) was added to a solution of 1-methylimidazole (8.21 g, 7.00 mL, 100 mmol, 2.0 equiv.) in THF (75 mL) at −60 °C over a period of 30 min. After an additional 30 min of stirring at this temperature, diethyl carbonate (5.91 g, 6.1 mL, 50 mmol, 1.0 equiv.) was added dropwise to the reaction mixture. Afterwards, the suspension was warmed to room temperature, stirred overnight, and then demineralised water (150 mL) was added to quench the reaction. The resulting suspension was extracted with dichloromethane (6 × 50 mL), the combined organic layers were dried with $MgSO_4$, and the remaining solvent was removed under reduced pressure. Colourless block-shaped crystals were obtained in 47 % yield (4.44 g, 23.3 mmol) upon recrystallisation from acetone. $C_9H_{10}N_4O$ (190.2): calcd. C 56.83, H 5.30, N 29.46; found C 56.55, H 5.20, N 29.70. ^{1}H NMR (300 MHz, [D_6]DMSO): δ = 7.52 (d, $^{3}J_{H,H}$ = 0.8 Hz, 2 H, H2), 7.12 (d, $^{3}J_{H,H}$ = 0.9 Hz, 2 H, H3), 3.89 (s, 6 H, H4) ppm. $^{13}C\{^{1}H\}$ NMR (75 MHz, [D_6]DMSO): δ = 174.25 (s, 1 C, C1′), 142.97 (s, 2 C, C1), 129.05 (s, 2 C, C3), 127.25 (s, 2 C, C2), 35.16 (s, 2 C, C4) ppm. EI-MS: *m/z* (%) = 190 (100) $[M]^{+}$, 175 (8) [M – Me]$^{+}$, 161 (80) [M – 2 Me]$^{+}$, 109 (97) [M – 1-MeNCNC$_2$H$_2$]$^{+}$.

(1-MeNCNC$_2$H$_2$)$_2$CH$_2$ (1): Hydrazine hydrate (35 % aqueous solution, 48.3 mL, 540 mmol, 34.0 equiv.) was added to a mixture of **1a** (3.00 g, 15.8 mmol, 1.0 equiv.) and KOH (3.00 g, 53.5 mmol, 3.4 equiv.), and the reaction solution was stirred at 150 °C for 3 h. After cooling to room temperature, the resulting solution was extracted with dichloromethane (3 × 40 mL), and the combined organic layers were washed with demineralised water (2 × 15 mL) to remove the remaining hydrazine. The organic layers were dried with $MgSO_4$, and the residual solvent was removed under reduced pressure. A pale-brown powder was obtained in 98 % yield (2.72 g, 15.4 mmol). $C_9H_{12}N_4$ (176.2): calcd. C 61.34, H 6.86, N 31.79; found C 60.35, H 6.60, N 31.45. ^{1}H NMR (300 MHz, [D_8]THF): δ = 6.79 (d, $^{3}J_{H,H}$ = 1.1 Hz, 2 H, H2), 6.71 (d, $^{3}J_{H,H}$ = 1.2 Hz, 2 H, H3), 4.12 (s, 6 H, H1′), 3.65 (s, 6 H, H4) ppm. $^{13}C\{^{1}H\}$ NMR (75 MHz, [D_8]THF): δ = 144.85 (s, 1 C, C1), 127.70 (s, 2 C, C3), 121.74 (s, 2 C, C2), 33.01 (s, 2 C, C4), 27.06 (s, 1 C, C1′) ppm. EI-MS: *m/z* (%) = 176 (100) $[M]^{+}$, 161 (23) [M – Me]$^{+}$, 95 (52) [M – 1-MeNCNC$_2$H$_2$]$^{+}$, 81(10) [1-MeNCNC$_2$H$_2$]$^{+}$.

(1-MeNCNC$_6$H$_4$)$_2$CH$_2$ (2): A solution of *N*-methyl-*ortho*-phenylenediamine (13.4 g, 12.5 mL, 110 mmol, 2.0 equiv.) and diethyl malonate (8.81 g, 8.3 mL, 55 mmol, 1.0 equiv.) in aqueous HCl (6 M, 150 mL) was heated to 120 °C and stirred for 2 d. Afterwards, the volume of the reaction mixture was reduced to half of its volume, and the pH value was adjusted to 10 by stepwise addition of aqueous ammonia solution (25 %). The resulting precipitate was filtered off and purified by column chromatography [acetone/Et_2O (1:1) + $HNEt_2$ (5 %)] and by recrystallisation from acetone. Compound **2** was isolated as pale-pink crystals (2.22 g, 8.0 mmol, 26 %). $C_{17}H_{16}N_4$ (276.3): calcd. C 73.89, H 5.84, N 20.27; found C 73.00, H 5.73, N 20.48. ^{1}H NMR (300 MHz, [D_8]THF): δ = 7.58–7.53 (m, 2 H, H3), 7.35–7.30 (m, 2 H, H6), 7.18–7.07 (m, 4 H, H4 + H5), 4.63 (s, 2 H, H1′), 3.92 (s, 6 H, H8) ppm. $^{13}C\{^{1}H\}$ NMR (75 MHz, [D_8]THF): δ = 150.90 (s, 1 C, C1), 144.03 (s, 2 C, C7), 137.45 (s, 2 C, C2), 122.71 (s, 2 C, C4), 122.11 (s, 2 C, C5), 120.04 (s, 2 C, C6), 110.02 (s, 2 C, C3), 30.43 (s, 2 C, C8), 28.32 (s, 1 C, C1′) ppm. EI-MS: *m/z* (%) = 276 (100) $[M]^{+}$, 261 (12) [M – Me]$^{+}$, 145 (36) [M – 1-MeNCNC$_6$H$_4$]$^{+}$, 131(14) [1-MeNCNC$_6$H$_4$]$^{+}$.

(NCSC$_6$H$_4$)CH$_2$(NCOC$_6$H$_4$) (3): 2-(Benzothiazol-2-yl)acetonitrile (12.86 g, 74.0 mmol, 1.00 equiv.), 2-aminophenol (8.08 g, 74.0 mmol, 1.00 equiv.) and polyphosphoric acid (80 %, ca. 250 mL) were heated to 185 °C while being vigorously stirred with a sealed preci-

sion glass (KPG) stirrer under an inert gas for an additional 7 h to complete the cyclisation reaction. Afterwards, it was cooled to approximately 80 °C, then poured onto ice and stirred overnight. The resulting brown solid was filtered, washed several times with demineralised water (6 × 100 mL) and saturated aqueous $NaHCO_3$ solution (3 × 30 mL) until pH neutrality was achieved. The desired product **3** was obtained as a brown powder (17.5 g, 65.7 mmol, 89 %). $C_{15}H_{10}N_2OS$ (266.32): calcd. C 67.65, H 3.78, N 10.52, S 12.04; found C 67.42, H 3.78, N 10.39, S 12.29. ^{1}H NMR (300 MHz, [D$_8$]THF): δ = 7.99–7.90 (m, 2 H, H3 + H6), 7.73–7.65 (m, 1 H, H13), 7.59–7.51 (m, 1 H, H10), 7.49–7.41 (m, 1 H, H5), 7.40–7.28 (m, 3 H, H4 + H11 + H12), 4.85 (s, 2 H, H1′) ppm. ^{13}C{^{1}H} NMR (75 MHz, [D$_8$]THF): δ = 164.62 (s, 1 C, C1), 163.00 (s, 1 C, C8), 154.37 (s, 1 C, C7), 152.27 (s, 1 C, C9), 142.69 (s, 1 C, C14), 137.06 (s, 1 C, C2), 126.82 (s, 1 C, C5), 126.00 (s, 1 C, C4), 125.86 (s, 1 C, C11), 125.15 (s, 1 C, C12), 123.93 (s, 1 C, C6), 122.47 (s, 1 C, C3), 120.83 (s, 1 C, C13), 111.29 (s, 1 C, C10), 34.38 (s, 1 C, C1′) ppm. ^{15}N{^{1}H} NMR (30 MHz, [D$_8$]THF): δ = –64.40 (s, N1), –132.37 (s, N2) ppm. EI-MS: *m/z* (%) = 266 (100) [M]$^+$, 148 (15) [M – $NCOC_6H_4$]$^+$.

($NCSC_6H_4$)CH_2(1-MeNCNC_6H_4) (4): 2-(Benzothiazol-2-yl)acetonitrile (2.82 g, 17.6 mmol, 1.00 equiv.), *N*-methyl-*ortho*-phenylenediamine (2.16 g, 2.0 mL, 17.6 mmol, 1.00 equiv.) and polyphosphoric acid (80 %, ca. 40 mL) were heated to 185 °C while being vigorously stirred with a sealed precision glass (KPG) stirrer for 7 h. Afterwards, it was cooled to approximately 80 °C, then poured onto ice and stirred for an additional hour1 h. The resulting green solid was filtered, washed twice with demineralised water (2 × 50 mL) and saturated aqueous $NaHCO_3$ solution (3 × 50 mL) until pH neutrality was achieved. Compound **3** was obtained as a green powder (2.35 g, 8.4 mmol, 48 %), and crystals suitable for X-ray diffraction experiments were grown from ethanol. $C_{16}H_{13}N_3S$ (279.36): calcd. C 68.79, H 4.69, N 15.04, S 11.48; found C 67.23, H 4.76, N 14.72, S 11.71. ^{1}H NMR (300 MHz, [D$_8$]THF): δ = 7.92 (d, $^3J_{H,H}$ = 8.1 Hz, 2 H, H6), 7.88 (d, $^3J_{H,H}$ = 7.9 Hz, 2 H, H3), 7.64–7.56 (m, 1 H, H13), 7.45–7.29 (m, 3 H, H4 + H5 + H10), 7.22–7.11 (m, 2 H, H11 + H12), 4.80 (s, 2 H, H1′), 3.83 (s, 3 H, H15) ppm. ^{13}C{^{1}H} NMR (75 MHz, [D$_8$]THF): δ = 167.44 (s, 1 C, C1), 154.39 (s, 1 C, C7), 151.16 (s, 1 C, C8), 144.17 (s, 1 C, C14), 137.41 (s, 1 C, C9), 137.07 (s, 1 C, C2), 126.64 (s, 1 C, C5), 125.80 (s, 1 C, C4), 123.69 (s, 1 C, C6), 122.88 (s, 1 C, C3), 122.45 (s, 1 C, C11), 122.25 (s, 1 C, C12), 120.33 (s, 1 C, C13), 110.10 (s, 1 C, C10), 33.76 (s, 1 C, C1′), 30.33 (s, 1 C, C15) ppm. ^{15}N{^{1}H} NMR (30 MHz, [D$_8$]THF): δ = –67.71 (s, N1), –132.50 (s, N2), –240.63 (s, N3) ppm. EI-MS: *m/z* (%) = 279 (100) [M]$^+$, 149 (11) [M – 1-MeNCNC_6H_4]$^+$, 131 (36) [1-MeNCNC_6H_4]$^+$.

Metallation Reactions

[Me_2Al{(1-MeNCNC_2H_2)$_2$CH}] (5): Pure $AlMe_3$ (0.23 mL, 165 mg, 2.40 mmol, 1.2 equiv.) was slowly added to a solution of **1** (352 mg, 2.00 mmol, 1.0 equiv.) in toluene (40 mL) at room temperature, and the clear reaction mixture was stirred overnight. Afterwards, the volume of the solution was reduced to a few mL, and the resulting concentrated solution was stored at –32 °C in a freezer. Crystals suitable for X-ray diffraction experiments were obtained overnight. The crystals thus formed were filtered, washed twice with precooled toluene and finally dried in vacuo. Colourless, block-shaped crystals were obtained in 20 % yield (92 mg, 0.40 mmol). $C_{11}H_{17}AlN_4$ (232.27): calcd. C 56.88, H 7.38, N 24.12; found C 56.52, H 7.76, N 24.36. ^{1}H NMR (400 MHz, [D$_8$]THF): δ = 6.54 (m, 2 H, H2), 6.52 (m, 2 H, H3), 4.06 (s, 1 H, H1′), 3.28 (s, 6 H, H7), –0.85 (s, 6 H, H1M) ppm. ^{13}C{^{1}H} NMR (75 MHz, [D$_8$]THF): δ = 153.92 (s, 2 C, C1), 118.32 (s, 2 C, C3), 117.45 (s, 2 C, C2), 50.46 (s, 1 C, C1′), 32.07 (s, 2 C, C7), –9.59 (s, 2 C, C1M) ppm. ^{15}N{^{1}H} NMR (50 MHz, [D$_8$]THF): δ = –222.08 (s, N2), –255.73 (s, N1) ppm. ^{27}Al{^{1}H} NMR (78 MHz, [D$_8$]THF): δ = 149 (s, Al1) ppm. EI-MS: *m/z* (%) = 176 (100) [M – $AlMe_2$]$^+$, 95 (77) [M – $AlMe_2$ – 1-MeNCNC_2H_2]$^+$, 81 (18) [1-MeNCNC_2H_2]$^+$.

[Me_2Al{(1-MeNCNC_6H_4)$_2$CH}] (6): Pure $AlMe_3$ (0.23 mL, 165 mg, 2.40 mmol, 1.2 equiv.) was slowly added to a solution of **2** (352 mg, 2.00 mmol, 1.0 equiv.) in toluene (40 mL) at room temperature, and the clear reaction mixture was stirred overnight. Afterwards, the volume of the solution was reduced to a few mL, and the resulting concentrated solution was stored at –32 °C in a freezer. The crystals thus formed were filtered, washed twice with precooled toluene and finally dried in vacuo. Colourless, needle-shaped crystals were obtained in 44 % yield (72 mg, 0.22 mmol). ^{1}H NMR (300 MHz, [D$_8$]THF): δ = 7.35–7.28 (m, 2 H, H6), 7.18–7.11 (m, 2 H, H3), 7.10–7.02 (m, 4 H, H3 + H4), 4.72 (s, 1 H, H1′), 3.57 (s, 6 H, H15), –0.57 (s, 6 H, H1M) ppm. ^{13}C{^{1}H} NMR (75 MHz, [D$_8$]THF): δ = 156.98 (s, 2 C, C1), 139.32 (s, 2 C, C7), 135.98 (s, 2 C, C2), 122.33 (s, 2 C, C5), 121.47 (s, 2 C, C4), 112.58 (s, 2 C, C6), 108.07 (s, 2 C, C3), 55.41 (s, 1 C, C1′), 29.09 (s, 2 C, C15), –9.85 (s, 2 C, C1M) ppm.

[Me_2Al{($NCSC_6H_4$)CH($NCOC_6H_4$)}] (7): A slight excess of pure $AlMe_3$ (0.22 mL, 158 mg, 2.20 mmol, 1.1 equiv.) was slowly added to a solution of **3** (0.533 g, 2.00 mmol, 1.0 equiv.) in toluene (40 mL) at 0 °C. The reaction mixture was stirred overnight and warmed to room temperature. The reaction mixture afforded a clear solution. Afterwards, the volume of the solution was reduced to a few mL, and the resulting concentrated solution was stored at –32 °C in a freezer. Crystals suitable for X-ray diffraction experiments were obtained overnight. The crystals thus formed were filtered, washed twice with precooled toluene and finally dried in vacuo. Compound **6** was isolated in the form of orange crystals (455 mg, 1.41 mmol, 71 %). $C_{17}H_{15}AlN_2OS$ (322.36): calcd. C 63.34, H 4.69, N 8.69, S 9.95; found C 63.26, H 4.78, N 8.54, S 9.77. ^{1}H NMR (500 MHz, [D$_8$]THF): δ = 7.69 (ddd, $J_{H,H}$ = 7.9, 1.3, 0.6 Hz, 1 H, H3), 7.58 (ddd, $J_{H,H}$ = 8.2, 1.0, 0.6 Hz, 1 H, H6), 7.42 (ddd, $J_{H,H}$ = 8.0, 1.1, 0.6 Hz, 1 H, H10), 7.42 (ddd, $J_{H,H}$ = 7.9, 1.2, 0.6 Hz, 1 H, H13), 7.39 (ddd, $J_{H,H}$ = 8.2, 7.3, 1.3 Hz, 1 H, H5), 7.29 (td, $J_{H,H}$ = 7.7, 1.1 Hz, 1 H, H12), 7.20 (ddd, $J_{H,H}$ = 7.9, 7.6, 1.2 Hz, 1 H, H11), 7.19 (ddd, $J_{H,H}$ = 7.9, 7.4, 1.0 Hz, 1 H, H4), 5.76 (s, 1 H, H1′), –0.45 (s, 6 H, H1M) ppm. ^{13}C{^{1}H} NMR (75 MHz, [D$_8$]THF): δ = 170.57 (s, 1 C, C8), 166.62 (s, 1 C, C1), 149.08 (s, 1 C, C9), 149.05 (s, 1 C, C7), 137.74 (s, 1 C, C14), 129.55 (s, 1 C, C2), 127.55 (s, 1 C, C5), 125.79 (s, 1 C, C12), 124.07 (s, 1 C, C4/C11), 123.87 (s, 1 C, C4/C11), 122.52 (s, 1 C, C3), 115.93 (s, 1 C, C6), 113.70 (s, 1 C, C13), 110.74 (s, 1 C, C10), 71.35 (s, 1 C, C1′), –9.78 (s, 2 C, C1M) ppm. ^{15}N{^{1}H} NMR (50 MHz, [D$_8$]THF): δ = –202.16 (s, N1), –228.74 (s, N2) ppm. ^{27}Al{^{1}H} NMR (78 MHz, [D$_8$]THF): δ = 151 (s, Al1) ppm. EI-MS: *m/z* (%) = 266 (100) [M – $AlMe_2$]$^+$, 148 (24) [M – $AlMe_2$ – $NCOC_6H_4$]$^+$.

[Me_2Ga{($NCSC_6H_4$)CH($NCOC_6H_4$)}] (8): Pure $GaMe_3$ (0.11 mL, 126 mg,1.10 mmol, 1.1 equiv.) was slowly added to a solution of **3** (0.266 g, 1.00 mmol, 1.0 equiv.) in toluene (20 mL) at 0 °C. The reaction mixture was stirred overnight and warmed to room temperature. Afterwards, the volume of the solution was reduced to a few mL, and the resulting concentrated solution was stored at –32 °C in a freezer. Crystals suitable for X-ray diffraction experiments were obtained overnight. The crystals thus formed were filtered, washed twice with precooled toluene and finally dried in vacuo. Compound **7** was isolated in the form of dark-orange crystals (184 mg, 0.50 mmol, 50 %). $C_{17}H_{15}GaN_2OS$ (365.10): calcd. C 55.92, H 4.14, N 7.67, S 8.78; found C 55.35, H 4.27, N 7.49, S 8.61. ^{1}H NMR (400 MHz, [D$_8$]THF): δ = 7.65 (ddd, $J_{H,H}$ = 7.9, 1.2, 0.6 Hz, 1 H, H3), 7.39 (ddd, $J_{H,H}$ = 8.2, 1.4, 0.6 Hz, 1 H, H6), 7.38 (ddd, $J_{H,H}$ = 8.0, 1.1, 0.6 Hz, 1 H, H10), 7.34 (ddd, $J_{H,H}$ = 8.2, 7.1, 1.2 Hz, 1 H, H5), 7.29 (ddd, $J_{H,H}$ = 7.8, 1.4, 0.6 Hz, 1 H, H13), 7.24 (ddd, $J_{H,H}$ = 7.8, 7.4, 1.1 Hz, 1 H, H12), 7.15 (ddd, $J_{H,H}$ = 8.0, 7.4, 1.4 Hz, 1 H, H11), 7.13

(ddd, $J_{H,H}$ = 7.9, 7.1, 1.4 Hz, 1 H, H4), 5.58 (s, 1 H, H1′), –0.03 (s, 6 H, H1M) ppm. $^{13}C\{^1H\}$ NMR (75 MHz, [D$_8$]THF): δ = 169.13 (s, 1 C, C8), 165.71 (s, 1 C, C1), 149.62 (s, 1 C, C7), 148.93 (s, 1 C, C9), 138.46 (s, 1 C, C14), 129.64 (s, 1 C, C2), 127.37 (s, 1 C, C5), 125.51 (s, 1 C, C12), 123.44 (s, 1 C, C4/C11), 123.30 (s, 1 C, C4/C11), 122.35 (s, 1 C, C3), 115.41 (s, 1 C, C6), 112.99 (s, 1 C, C13), 110.48 (s, 1 C, C10), 70.09 (s, 1 C, C1′), –6.97 (s, 2 C, C1M) ppm. $^{15}N\{^1H\}$ NMR (40 MHz, [D$_8$]THF): δ = –200.07 (s, N1), –228.48 (s, N2) ppm. EI-MS: *m/z* (%) = 364.0 (13) [M]$^+$, 349 (100) [M – Me]$^+$, 334 (27) [M – 2 Me]$^+$, 265 (9) [M – GaMe$_2$]$^+$, 69 (58) Ga$^+$.

[Me$_2$Al{(NCSC$_6$H$_4$)CH(1-MeNCNC$_6$H$_4$)}] (9): A solution of AlMe$_3$ (0.06 mL, 43 mg, 0.60 mmol, 1.2 equiv.) in toluene (5 mL) was added dropwise to a solution of **4** (140 mg, 0.50 mmol, 1.0 equiv.) in toluene (40 mL) at room temperature, and the clear reaction mixture was stirred overnight. Afterwards, the volume of the solution was reduced to a few mL, and the resulting concentrated solution was stored at –32 °C in a freezer. Crystals suitable for X-ray diffraction experiments were obtained overnight. The crystals thus formed were filtered, washed twice with precooled toluene and finally dried in vacuo. Compound **8** was isolated in the form of greenish crystals (49 mg, 0.15 mmol, 30 %, not optimised). $C_{18}H_{18}AlN_3S$ (335.40): calcd. C 64.46, H 5.41, N 12.53, S 9.56; found C 62.68, H 5.41, N 11.92, S 9.07. ^1H NMR (400 MHz, [D$_8$]THF): δ = 7.52 (ddd, $J_{H,H}$ = 7.8, 1.3, 0.6 Hz, 1 H, H3), 7.49–7.44 (m, 1 H, H13), 7.43 (ddd, $J_{H,H}$ = 8.1, 1.1, 0.6 Hz, 1 H, H6), 7.33–7.30 (m, 1 H, H10), 7.27 (ddd, $J_{H,H}$ = 8.1, 7.4, 1.3 Hz, 1 H, H5), 7.23–7.16 (m, 2 H, H11 + H12), 7.05 (ddd, $J_{H,H}$ = 7.8, 7.4, 1.1 Hz, 1 H, H4), 5.57 (s, 1 H, H1′), 3.63 (s, 3 H, H15), –0.50 (s, 6 H, H1M) ppm. $^{13}C\{^1H\}$ NMR (75 MHz, [D$_8$]THF): δ = 166.65 (s, 1 C, C1), 154.42 (s, 1 C, C8), 149.90 (s, 1 C, C7), 138.64 (s, 1 C, C14), 135.42 (s, 1 C, C9), 128.98 (s, 1 C, C2), 127.00 (s, 1 C, C5), 123.28 (s, 1 C, C12), 122.83 (s, 1 C, C11), 122.57 (s, 1 C, C4), 121.90 (s, 1 C, C3),

Table 4. Crystal structure data for **1**–**5** and **7**–**11**.

	1	**2**	**3**	**3a**	**4**·H$_2$O	**5**
Empirical formula	$C_9H_{12}N_4$	$C_{17}H_{16}N_4$	$C_{15}H_{10}N_2OS$	$C_{15}H_{12}N_2O_2S$	$C_{16}H_{11}N_3S{\cdot}H_2O$	$C_{11}H_{17}AlN_4$
Formula mass	176.23	276.34	266.31	284.33	297.37	232.26
Wavelength [Å]	0.71073	0.71073	0.71073	0.71073	0.71073	0.71073
Crystal system	tetragonal	triclinic	triclinic	orthorhombic	monoclinic	monoclinic
Space group	$P4_32_12$	$P\bar{1}$	$P\bar{1}$	$Pna2_1$	$P2_1$	$P2_1/c$
a [Å]	7.078(2)	8.292(2)	5.908(2)	22.104(3)	4.790(2)	13.500(3)
b [Å]	7.078(2)	8.395(2)	9.841(2)	4.695(2)	28.552(4)	17.133(4)
c [Å]	17.810(3)	10.543(3)	10.682(3)	12.588(2)	10.749(3)	12.370(3)
α [°]	90	68.80(2)	81.96(2)	90	90	90
β [°]	90	83.69(2)	87.52(3)	90	99.92(2)	117.14(2)
γ [°]	90	83.20(2)	81.07(2)	90	90	90
V [Å^3]	892.2(3)	677.6(3)	607.4(3)	1306.4(6)	1448.1(8)	2546.1(11)
Z	4	2	2	4	4	8
Reflections measured	26062	18451	20040	18979	24144	39111
Refllections unique	1367	3377	2588	3374	6106	4705
R_{int}	0.0461	0.0262	0.0221	0.0339	0.0294	0.0931
Data/restraints/parameters	1367/0/65	3380/0/192	2588/227/179	3374/3/189	6106/591/426	4705/393/299
*R*1 [$I > 2\sigma(I)$][a]	0.0334	0.0404	0.0297	0.0277	0.0304	0.0483
w*R*2 (all reflections)[b]	0.0916	0.1112	0.0755	0.0717	0.0719	0.1410
Absolute structure parameter[24]	not defined reliably	–	–	0.03(3)	0.21(7)	–
Extinction coefficient	–	–	–	–	–	0.0021(5)
$\Delta\varrho_{fin}$ [e Å^{-3}]	0.364/–0.190	0.356/–0.248	0.347/–0.343	0.294/–0.205	0.239/–0.227	0.395/–0.313

	7	**8**	**9**	**10**	**11**·4diox
Empirical formula	$C_{17}H_{15}AlN_2OS$	$C_{17}H_{15}GaN_2OS$	$C_{18}H_{18}AlN_3S$	$C_{25}H_{31}LiN_4O_2$	$C_{16}H_{12}LiN_3S{\cdot}4C_4H_8O_2$
Formula mass	322.35	365.09	335.39	426.48	637.70
Wavelength [Å]	0.71073	0.56086	0.71073	0.71073	0.71073
Crystal system	monoclinic	orthorhombic	monoclinic	monoclinic	monoclinic
Space group	$P2_1/c$	Pnma	$P2_1/m$	$P2_1/c$	$P2_1/c$
a [Å]	14.594(3)	8.262(2)	7.230(3)	21.030(2)	9.609(2)
b [Å]	7.086(2)	16.440(4)	14.864(4)	9.072(2)	12.915(3)
c [Å]	15.288(3)	11.473(3)	8.340(3)	23.894(2)	26.515(4)
β [°]	93.35(2)	90	112.67(2)	98.43(2)	95.94(3)
V [Å^3]	1578.3(6)	1558.3(7)	827.0(5)	4509.3(12)	3272.8(11)
Z	4	4	2	8	4
Reflections measured	25152	37294	9160	128019	51453
Reflections unique	2916	2464	2210	8298	7527
R_{int}	0.0543	0.0346	0.0310	0.0704	0.0583
Data/restraints/parameters	2916/287/221	2464/382/192	2210/398/201	8298/826/657	7527/3723/866
*R*1 [$I > 2\sigma(I)$][a]	0.0395	0.0490	0.0701	0.0387	0.0718
*wR*2 (all reflections)[b]	0.1037	0.1137	0.2016	0.0948	0.1507
Extinction coefficient	–	–	–	0.00165(18)	0.0018(3)
$\Delta\varrho_{fin}$ [e Å^{-3}]	0.338/–0.281	0.747/–0.883	0.754/–0.947	0.199/–0.187	0.242/–0.268

[a] $R1 = \frac{\Sigma||F_o| - |F_c||}{\Sigma|F_o|}$. [b] $wR2 = \sqrt{\frac{\sum w(F_o^2 - F_c^2)^2}{\sum w(F_o^2)^2}}$; $w = \frac{1}{(F_o^2) + (g_1P)^2 + g_2P}$; $P = \frac{(F_o^2 + 2F_c^2)}{3}$.

114.87 (s, 1 C, C6), 113.67 (s, 1 C, C13), 109.44 (s, 1 C, C10), 70.71 (s, 1 C, C1′), 29.35 (s, 1 C, C15), –9.58 (s, 2 C, C1M) ppm. $^{15}N\{^1H\}$ NMR (50 MHz, [D$_8$]THF): δ = –223.12 (s, N1), –226.41 (s, N3), –257.67 (s, N2) ppm. $^{27}Al\{^1H\}$ NMR (78 MHz, [D$_8$]THF): δ = 150 (s, Al1) ppm. EI-MS: *m/z* (%) = 335 (11) $[M]^+$, 320 (100) $[M - Me]^+$, 305 (19) $[M - 2\,Me]^+$, 160 (12) $[M - Me]^{2+}$.

[(THF)$_2$Li{(1-MeNCNC$_6$H$_4$)$_2$CH}] (10): At –60 °C, *n*BuLi (2.15 M in hexane, 0.72 mL, 1.44 mmol, 4.0 equiv.) was added slowly to a solution of **2** (100 mg, 0.36 mmol, 1.0 equiv.) in THF (10 mL), and the reaction mixture was stirred overnight. Afterwards, the volume of the solution was reduced to a few mL, and the resulting concentrated solution was stored at –32 °C in a freezer. Crystals suitable for X-ray diffraction experiments were obtained overnight. The crystals thus formed were filtered, and the remaining solvent was removed under reduced pressure. Yellow, plate-shaped crystals were obtained in 92 % yield (142 mg, 0.33 mmol). $C_{11}H_{17}AlN_4$ (232.27). ^1H NMR (400 MHz, [D$_8$]THF): δ = 7.02 (d, $^3J_{H,H}$ = 7.6 Hz, 2 H, H6), 6.85 (d, $^3J_{H,H}$ = 7.6 Hz, 2 H, H3), 6.79 (td, $J_{H,H}$ = 7.5, 1.2 Hz, 2 H, H5), 6.70 (td, $J_{H,H}$ = 7.5, 1.1 Hz, 2 H, H4), 4.23 (s, 1 H, H1′), 3.46 (s, 6 H, H8) ppm. $^{13}C\{^1H\}$ NMR (100 MHz, [D$_8$]THF): δ = 159.93 (s, 2 C, C1), 146.32 (s, 2 C, C7), 137.23 (s, 2 C, C2), 120.09 (s, 2 C, C5), 117.23 (s, 2 C, C4), 112.36 (s, 2 C, C6), 105.69 (s, 2 C, C3), 54.10 (s, 1 C, C1′), 28.91 (s, 2 C, C8) ppm. $^7Li\{^1H\}$ NMR (155 MHz, [D$_8$]THF): δ = 2.54 (s, Li1) ppm.

[(diox)$_2$Li{(NCSC$_6$H$_4$)CH(1-MeNCNC$_6$H$_4$)}] (11): At room temperature, *n*BuLi (2.93 M in hexane, 0.17 mL, 0.50 mmol, 1.0 equiv.) was slowly added to a suspension of **4** (140 mg, 0.50 mmol, 1.0 equiv.) in 1,4-dioxane (15 mL). The resulting brown suspension was stirred overnight and filtered to obtain a brown solution. Afterwards, the volume of the solution was reduced to a few mL, and the resulting concentrated solution was stored at room temperature. Crystals suitable for X-ray diffraction experiments were obtained after a week. The crystals thus formed were filtered and dried in vacuo. Yellow needles were isolated in 78 % yield (145 mg, 0.39 mmol, not optimised). $C_{20}H_{20}LiN_3OS$ (373.40): calcd. C 64.33, H 5.40, N 11.25, S 8.59; found C 60.33, H 6.50, N 7.95, S 6.64 (deviations due to remaining lattice solvent). ^1H NMR (400 MHz, [D$_8$]THF): δ = 7.30 (ddd, $J_{H,H}$ = 7.6, 1.3, 0.5 Hz, 1 H, H3), 7.12 (ddd, $J_{H,H}$ = 7.6, 1.3, 0.6 Hz, 1 H, H13), 7.09 (ddd, $J_{H,H}$ = 8.0, 1.2, 0.5 Hz, 1 H, H6), 7.01–6.96 (m, 2 H, H5 + H10), 6.89 (td, $J_{H,H}$ = 7.5, 1.4 Hz, 1 H, H12), 6.83 (td, $J_{H,H}$ = 7.5, 1.3 Hz, 1 H, H11), 6.68 (ddd, $J_{H,H}$ = 7.6, 7.3, 1.2 Hz, 1 H, H4), 4.95 (s, 1 H, H1′), 3.48 (s, 3 H, H15) ppm. $^{13}C\{^1H\}$ NMR (75 MHz, [D$_8$]THF): δ = 167.44 (s, 1 C, C1), 157.78 (s, 1 C, C7/C8), 157.64 (s, 1 C, C7/C8), 145.45 (s, 1 C, C14), 136.62 (s, 1 C, C9), 131.78 (s, 1 C, C2), 125.42 (s, 1 C, C5), 120.68 (s, 1 C, C12), 120.46 (s, 1 C, C3), 118.74 (s, 1 C, C4/C11), 118.73 (s, 1 C, C4/C11), 114.75 (s, 1 C, C6), 113.60 (s, 1 C, C13), 107.01 (s, 1 C, C10), 68.46 (s, 1 C, C1′), 28.98 (s, 1 C, C15) ppm. $^7Li\{^1H\}$ NMR (117 MHz, [D$_8$]THF): δ = 2.37 (s, Li1) ppm. $^{15}N\{^1H\}$ NMR (40 MHz, [D$_8$]THF): δ = –168.43 (s, N1), –190.35 (s, N3), –261.53 (s, N2) ppm. EI-MS: *m/z* (%) = 293 (13) $[M + Li]^+$, 279 (100) $[M - Li]^+$, 149 (18) $[M - Li - 1\text{-}MeNCNC_6H_4]^+$, 131 (57) $[1\text{-}MeNCNC_6H_4]^+$.

Crystallographic Details: Shock-cooled crystals were selected from a Schlenk line under argon using the X-TEMP2.[17] The data were integrated with SAINT,[18] and a multiscan absorption correction (SADABS)[19] and a 3λ correction were applied.[20] The structures were solved by direct methods (SHELXT)[21] and refined on F^2 using the full-matrix least-squares methods of SHELXL[22] within the SHELXLE GUI.[23] Crystal structure data for **1**–**5** and **7**–**11** are shown in Table 4. More details on the crystallographic data and the refinement can be found in the Supporting Information. CCDC 1521021 (for **1**), 1521022 (for **2**), 1521030 (for **3**), 1521025 (for **3a**), 1521031 (for **4**·H$_2$O), 1521023 (for **5**), 1521028 (for **7**), 1521029 (for **8**), 1521024 (for **9**), 1521026 (for **10**), 1521027 (for **11**·4diox) contain the supplementary crystallographic data for this paper. These data can be obtained free of charge from The Cambridge Crystallographic Data Centre.

Acknowledgments

Thanks to the Danish National Research Foundation (DNRF93) funded Center for Materials Crystallography (CMC) for partial support and the Federal State of Lower Saxony, Germany for providing fellowships in the GAUSS and CaSuS PhD programs.

Keywords: Organometallic synthesis · Aluminium · Gallium · Lithium · NacNac

[1] a) S. G. McGeachin, *Can. J. Chem.* **1968**, *46*, 1903–1912; b) R. Bonnett, D. C. Bradley, K. J. Fisher, *Chem. Commun. (London)* **1968**, 886–887; c) J. E. Parks, R. H. Holm, *Inorg. Chem.* **1968**, *7*, 1408–1416.

[2] a) M. Stender, B. E. Eichler, N. J. Hardman, P. P. Power, J. Prust, M. Noltemeyer, H. W. Roesky, *Inorg. Chem.* **2001**, *40*, 2794–2799; b) B. Qian, D. L. Ward, M. R. Smith, *Organometallics* **1998**, *17*, 3070–3076; c) S. Singh, H.-J. Ahn, A. Stasch, V. Jancik, H. W. Roesky, A. Pal, M. Biadene, R. Herbst-Irmer, M. Noltemeyer, H.-G. Schmidt, *Inorg. Chem.* **2006**, *45*, 1853–1860; d) Z. Yang, H. Zhu, X. Ma, J. Chai, H. W. Roesky, C. He, J. Magull, H.-G. Schmidt, M. Noltemeyer, *Inorg. Chem.* **2006**, *45*, 1823–1827; e) S. Nagendran, H. W. Roesky, *Organometallics* **2008**, *27*, 457–492; f) Y. Ding, H. W. Roesky, M. Noltemeyer, H.-G. Schmidt, P. P. Power, *Organometallics* **2001**, *20*, 1190–1194; g) A. Jana, H. W. Roesky, C. Schulzke, A. Döring, T. Beck, A. Pal, R. Herbst-Irmer, *Inorg. Chem.* **2009**, *48*, 193–197; h) Y. Cheng, D. J. Doyle, P. B. Hitchcock, M. F. Lappert, *Dalton Trans.* **2006**, 4449–4460; i) N. Kuhn, J. Fahl, S. Fuchs, M. Steimann, G. Henkel, A. H. Maulitz, *Z. Anorg. Allg. Chem.* **1999**, *625*, 2108–2114; j) N. Kuhn, S. Fuchs, M. Steimann, *Eur. J. Inorg. Chem.* **2001**, 359–361; k) N. Kuhn, S. Fuchs, M. Steimann, *Z. Anorg. Allg. Chem.* **2002**, *628*, 458–462; l) C. E. Radzewich, I. A. Guzei, R. F. Jordan, *J. Am. Chem. Soc.* **1999**, *121*, 8673–8674.

[3] a) D. Li, Y. Peng, C. Geng, K. Liu, D. Kong, *Dalton Trans.* **2013**, *42*, 11295–11303; b) Z. Yang, M. Zhong, X. Ma, S. De, C. Anusha, P. Parameswaran, H. W. Roesky, *Angew. Chem. Int. Ed.* **2015**, *54*, 10225–10229; *Angew. Chem.* **2015**, *127*, 10363–10367; c) Z. Yang, M. Zhong, X. Ma, K. Nijesh, S. De, P. Parameswaran, H. W. Roesky, *J. Am. Chem. Soc.* **2016**, *138*, 2548–2551; d) V. K. Jakhar, M. K. Barman, S. Nembenna, *Org. Lett.* **2016**, *18*, 4710–4713; e) A. Bismuto, S. P. Thomas, M. J. Cowley, *Angew. Chem. Int. Ed.* **2016**, *55*, 15356–15359; *Angew. Chem.* **2016**, *128*, 15582–15585.

[4] a) D.-R. Dauer, D. Stalke, *Dalton Trans.* **2014**, *43*, 14432–14439; b) D.-R. Dauer, M. Flügge, R. Herbst-Irmer, D. Stalke, *Dalton Trans.* **2016**, *45*, 6149–6158; c) D.-R. Dauer, M. Flügge, R. Herbst-Irmer, D. Stalke, *Dalton Trans.* **2016**, *45*, 6136–6148.

[5] H. Schödel, C. Näther, H. Bock, F. Butenschön, *Acta Crystallogr., Sect. B: Struct. Sci.* **1996**, *52*, 842–853.

[6] a) H. Gornitzka, D. Stalke, *Angew. Chem. Int. Ed. Engl.* **1994**, *33*, 693–695; *Angew. Chem.* **1994**, *106*, 695–698; b) H. Gornitzka, D. Stalke, *Organometallics* **1994**, *13*, 4398–4405; c) H. Gornitzka, C. Hemmert, G. Bertrand, M. Pfeiffer, D. Stalke, *Organometallics* **2000**, *19*, 112–114; d) T. Kottke, D. Stalke, *Chem. Ber./Recl.* **1997**, *130*, 1365–1374.

[7] L. Mahalakshmi, D. Stalke in *Structure and Bonding*, vol. 103 ("Group 13 Chemistry I") (Eds.: H. W. Roesky, D. A. Atwood), Springer, Berlin, **2002**, pp. 85–115.

[8] P. Vasko, V. Kinnunen, J. O. Moilanen, T. L. Roemmele, R. T. Boere, J. Konu, H. M. Tuononen, *Dalton Trans.* **2015**, *44*, 18247–18259.

[9] a) C. Rai, J. B. Braunwarth, *J. Org. Chem.* **1961**, *26*, 3434–3436; b) W. H. Mills, *J. Chem. Soc. Trans.* **1922**, *121*, 455–466.

[10] a) C. Avendaño, M. T. Ramos, J. Elguero, M. L. Jimeno, J. Bellanato, F. Florencio, *Can. J. Chem.* **1988**, *66*, 1467–1473; b) T. Ramos, C. Avendaño, J. Elguero, *J. Heterocycl. Chem.* **1987**, *24*, 247–249.

[11] a) A. Abbotto, S. Bradamante, A. Facchetti, G. A. Pagani, *J. Org. Chem.* **2002**, *67*, 5753–5772; b) A. Abbotto, S. Bradamante, G. A. Pagani, *J. Org.*

Chem. **1996**, *61*, 1761–1769; c) A. Abbotto, S. Bradamante, N. Capri, H. Rzepa, D. J. Williams, A. White, *J. Org. Chem.* **1996**, *61*, 1770–1778.
[12] a) S. Bradamante, G. A. Pagani, *J. Org. Chem.* **1984**, *49*, 2863–2870; b) A. Abbotto, V. Alanzo, S. Bradamante, G. A. Pagani, *J. Chem. Soc. Perkin Trans. 2* **1991**, 481–488; c) C. Gatti, A. Ponti, A. Gamba, G. Pagani, *J. Am. Chem. Soc.* **1992**, *114*, 8634–8644; d) A. Abbotto, S. Bradamante, G. A. Pagani, *J. Org. Chem.* **1993**, *58*, 444–448; e) F. Ragaini, M. Pizzotti, S. Cenini, A. Abbotto, G. A. Pagani, F. Demartin, *J. Organomet. Chem.* **1995**, *489*, 107–112; f) A. Abbotto, A. Facchetti, S. Bradamante, G. A. Pagani, *J. Org. Chem.* **1998**, *63*, 436–444; g) S. Bradamante, G. A. Pagani, *J. Chem. Soc. Perkin Trans. 2* **1986**, 1035–1046.
[13] a) E. Arunan, G. R. Desiraju, R. A. Klein, J. Sadlej, S. Scheiner, I. Alkorta, D. C. David, R. H. Crabtree, J. J. Dannenberg, P. Hobza, H. G. Kjaergaard, A. C. Legon, B. Mennucci, D. J. Nesbitt, *Pure Appl. Chem.* **2011**, *83*, 1637; b) G. R. Desiraju, *Acc. Chem. Res.* **2002**, *35*, 565–573; c) T. Steiner, *Angew. Chem. Int. Ed.* **2002**, *41*, 48–76; *Angew. Chem.* **2002**, *114*, 50–80; d) D. Braga, F. Grepioni, G. R. Desiraju, *Chem. Rev.* **1998**, *98*, 1375–1406; e) J. Emsley, *Chem. Soc. Rev.* **1980**, *9*, 91–124; f) G. A. Jeffrey, W. Saenger, *Hydrogen Bonding in Biological Structures*, Springer, Berlin, **1991**; g) G. A. Jeffrey, *An Introduction to Hydrogen Bonding*, Oxford University Press, New York, **1997**; h) J. Overgaard, B. B. Iversen in *Structure and Bonding*, vol. 146 ("Electron Density and Chemical Bonding 1") (Ed.: D. Stalke), Springer, Berlin, **2012**, pp. 53–74.
[14] D. R. Lide, *CRC Handbook of Chemistry and Physics: A Ready-Reference Book of Chemical and Physical Data*, CRC Press, Boca Raton, **2006**.
[15] Schlenk techniques, http://www.stalke.chemie.uni-goettingen.de/virtuelles_labor/advanced/13_de.html.
[16] NMR spectroscopy, http://www.stalke.chemie.uni-goettingen.de/virtuelles_labor/nmr/de.html.
[17] a) T. Kottke, D. Stalke, *J. Appl. Crystallogr.* **1993**, *26*, 615–619; b) D. Stalke, *Chem. Soc. Rev.* **1998**, *27*, 171–178.
[18] Bruker AXS Inc., *Bruker Apex CCD, SAINT v8.30C*, Bruker AXS Inst. Inc., Madison, **2013**.
[19] L. Krause, R. Herbst-Irmer, G. M. Sheldrick, D. Stalke, *J. Appl. Crystallogr.* **2015**, *48*, 3–10.
[20] L. Krause, R. Herbst-Irmer, D. Stalke, *J. Appl. Crystallogr.* **2015**, *48*, 1907–1913.
[21] G. M. Sheldrick, *Acta Crystallogr., Sect. A: Found. Crystallogr.* **2015**, *71*, 3–8.
[22] G. M. Sheldrick, *Acta Crystallogr., Sect. C: Struct. Chem.* **2015**, *71*, 3–8.
[23] C. B. Hübschle, B. Dittrich, *J. Appl. Crystallogr.* **2011**, *44*, 238–240.
[24] S. Parsons, H. D. Flack, T. Wagner, *Acta Crystallogr., Sect. B: Struct. Sci. Cryst. Eng. Mater.* **2013**, *69*, 249–259.

Received: December 8, 2016

